Detecting Cognitive State Changes by Learning Task-Specific Functional Connectivity Fingerprint

Authors

Affiliations

Abstract. Functional resonance magnetic imaging (fMRI) technology has been widely used in understanding the fundamental mechanism of psychophysiological processes by investigating the functional interaction between distant brain regions. Since the behavior of functional connectivity often dynamically shifts along with the change of cognitive states, it is challenging to characterize the dynamic behavior in connectivity without requiring prior knowledge of experiment settings. To address this challenge, we present a change point detection network (CPD-Net) solution to automatically detect state changes on an individual basis. The input includes a set of functional connectivity (FC) matrices captured along the sliding windows. To respect the intrinsic geometry in FC matrix, we first deploy a deep neural network to learn the low-dimension feature representation (called FC fingerprint) on a Riemannian manifold of SPD (symmetric positive definite) matrix. After that, the learned FC fingerprints are used to stratify the sliding windows in the feed-forward process through a deep recurrent mean-shift network. In the back-propagation stage, the possible mis-stratification of brain states is used to steer the representation learning of FC fingerprints, where the updated FC fingerprints have more and more discriminating power to distinguish the underlying functional task against others. We have conducted our CPD-Net on both simulated data and task-based fMRI data from HCP (human connectome project) database. We also have evaluated the accuracy, replicability, and scalability of change detection, where we achieve more accurate and consistent results than current learning-based CPD methods.

Keywords: Deep Neural Network, Symmetric Positive Definite Matrix, Mean Shift, Change Detection, Functional MRI.

1 Introduction

In the neuroscience field, one of the fundamental scientific problems is to understand how cognition and behavior emerge from brain function. In the last couple of decades, striking efforts have been made to deliver structural and functional brain mapping *in-vivo* using cutting-edge neuroimaging technology. For instance, we can investigate the functional interactions between spatially distinct brain regions using fMRI [1], where we used to study them separately.

Recently, the research focus of fMRI studies has been shifted to functional dynamics since the cognitive states frequently vary even in a short period of resting time [2]. In

addition, mounting evidence indicates that the dynamic behavior of functional connectivity is more closely associated with the development of neurological diseases. In light of this, characterizing functional dynamics from the observed BOLD (blood-oxygen-level-dependent) signals becomes an important step to understand the psychophysiological mechanism of cognition and discover disease-relevant neuroimaging biomarkers. Due to the practical limitations in fMRI, such as low signal-to-noise level and the indirect proxy of neural activity, it is difficult to detect the change of cognitive states without knowing the setting of tasks in fMRI experiments.

To address this challenge, various change point detection (CPD) approaches have been proposed in the literature. Generally speaking, current state-of-the-art change detection methods can be categorized into either supervised or unsupervised scenarios. Regarding the supervised CPD methods, the learning component is often trained to establish the mapping between the functional neuroimaging data and the cognitive states. For example, the Bayesian-based statistical inference has been used to partition the time course into segments by modeling the statistics of BOLD signals and the temporal transition probability [3, 4]. A recurrent neural network (RNN) has been proposed in [5] by considering the brain state change detection as a classification problem where the RNN is trained to predict the task label based on the FC signatures vectors generated through non-negative matrix decomposition [6].

Regarding the unsupervised CPD approach, it is a common practice to cast the change detection into a data clustering process. The working premise is that time points associated with the same functional tasks are supposed to fall into the same cluster. Although most of the current unsupervised CPD methods adapt the clustering technique in computer vision and machine learning areas, many efforts have been made to contrive the putative and low-dimensional feature representation for each time point, which describes the functional connectivity profile within the underlying sliding window. For example, the FC matrix in each sliding window is often vectorized into a data array and then stratified into several groups using classic clustering techniques, such as k-means and locally linear embedding (LLE) [7]. By doing so, the whole scanning period can be partitioned into several segments, where each segment is supposed to correspond to a specific cognitive task during fMRI scan. Recently, the graph learning technique has been proposed to construct the subspace of individual fMRI data, which is jointly spanned by Fourier bases and the Eigen bases of graph Laplacian [8]. After that, the spectrum coefficients after projecting BOLD time course into the learned subspace are used to stratify time points into different clusters.

The functional brain network is fundamentally a covariance matrix often assessed by statistical measures such as correlation [9]. In this context, FC matrix essentially resides on a Riemannian manifold of SPD matrix. Despite the rich mathematical insight of SPD manifold, such intrinsic geometry of functional network data is not well investigated in functional brain network analysis, including the state change point detection. In this paper, we present a deep neural network (called CPD-Net) to (1) learn the low-dimensional FC fingerprint on the SPD manifold and (2) stratify the time points into different functional tasks through a sequence of learned mean-shift kernels. Specifically, the input to our CPD-Net is a set of FC matrices calculated in each sliding window (centered at the underlying time point). To perverse the intrinsic geometry in

FC matrices, we adapt a manifold-based convolutional neural network (CNN) to boil down the FC matrices from high-dimensional SPD manifold to the FC fingerprints in a low-dimensional vector space (displayed in **Fig. 1(d)**). Furthermore, we integrate a recurrent neural network (RNN) of mean-shift to find the modes of leaned FC fingerprints (**Fig. 1(e)**), where the difference between identified modes and brain states (ground truth) is used to steer the feature representation learning and kernel density estimation in the iterative process of mean-shift (**Fig. 1(f)**).

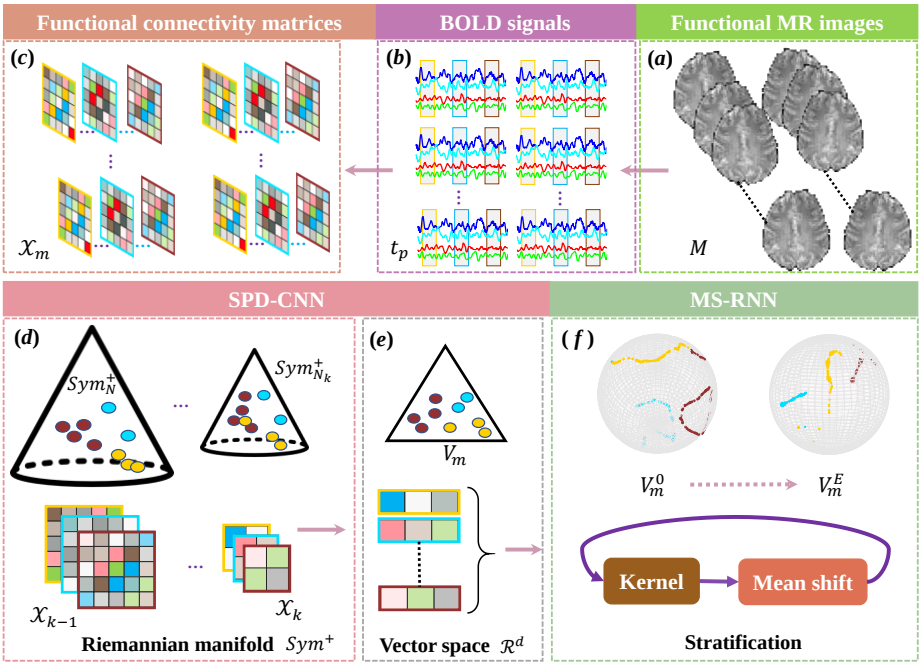

Fig. 1. Overview of our CPD-Net. The input to our CPD-Net is a set of FC matrices (c), which is constructed using the sliding window technique, based on the mean time course of BOLD signal (b) from task fMRI scans (a). First, we learn the feature representations on the Riemannian manifold of SPD matrix through a manifold-based CNN (d), which yields a set of low-dimension FC fingerprints in the vector space (e). Next, we integrate an RNN of mean shift (f) to group the FC fingerprints into the associated task stratification. Since the possible mis-stratification is eventually back-propagated to the neural network of feature representation learning to refine the task-specific FC fingerprints, our CPD-Net offers an integrated supervised learning solution offers to detect brain state changes.

The most relevant work is a Riemannian metric presented in [10], where the distance between two fMRI scans is measured by the geodesic between two trajectories of SPD matrices on SPD manifold. Our proposed CPD-Net is enlightened by two machine learning components in the computer vision area: the Riemannian network [11] for learning features on SPD manifold and the recurrent pixel embedding learning for instance grouping [12]. Based on these existing works, our CPD-Net has two major

contributions. (1) We present a novel integrated solution to simultaneously infer task-specific feature representations and detect state changes, compared to the current approaches where the feature learning and change detection are often performed in two steps separately. (2) To our knowledge, our work is the first attempt to detect the change of brain states using the manifold-based neural network.

We have evaluated our CPD-Net on both simulated data and working memory fMRI data from HCP database. Compared to the current learning-based CPD methods, our CPD-Net achieves more accurate detection results with the enhanced replicability on the test-retest experiments, which indicates the great applicability of our CPD-Net in neuroscience studies.

2 Method

Suppose the training data consist of M task fMRI scans (**Fig.1 (a)**). Each scan has been processed into N mean time courses of BOLD signal with P time points (**Fig.1 (b)**), where N denotes the number of brain parcellations. We use the sliding window technique to capture functional dynamics. Specifically, we construct the $N \times N$ FC matrix at the underlying time point t_p ($p = 1, \dots, P$) based on the BOLD signal within the time window w_p, where the sliding window center is t_p. Thus, the functional dynamics for each scan can be encoded in a sequence of FC matrices $\mathbb{X}_m = \{\mathcal{X}_m(t_p) | p = 1, \dots, P\}$ ($m = 1, \dots, M$), as shown in **Fig. 1(c)**.

There are Q cognitive tasks $\Gamma = \{\gamma_q | q = 1, \dots, Q\}$ in each scan. Since we know the functional task schedule of fMRI scan for training data, we can associate each $\mathcal{X}_m(t_p)$ with a task label $y_m(t_p) \in \Gamma$. In this paper, we present our CPD-Net to predict the stratification result based on the temporal-evolving FC matrices of the new instance of fMRI scan. The overall network architecture is shown in **Fig. 1(d)-(f)**, which consists of two major learning components described below.

2.1 Neural network of SPD manifold for feature representation learning

To preserve the intrinsic geometric properties of FC matrix, we adapt a Riemannian network [11] to (1) learn the low-dimensional feature representation on the Riemannian manifold of SPD matrix, and (2) project each FC matrix from the Riemannian manifold into a vector space which allows us to stratify functional tasks using the classic Euclidean operations.

In a nutshell, the Riemannian network for SPD matrix learning in [11] works the sense of convolutional neural network, except the convolution and ReLU (rectified linear units) operations in CNN have been replaced with manifold algebra. In what follows, we use $\mathcal{F}_\Theta(\mathcal{X})$ to denote the SPD-CNN (with the network parameters Θ) for inferring the task-specific feature vector $v \in \mathcal{R}^d$ from the high dimensional input $\mathcal{X} \in Sym_N^+$, where Sym_N^+ stands for the Riemannian manifold of $N \times N$ SPD matrices. Since we apply the same SPD-CNN $\mathcal{F}_\Theta$ to all $\mathcal{X}_m(t_p)$ one after another, we drop the variable t_p (for time) and subscript m (for subject) in Section 2.1, for clarity.

As shown in **Fig. 1(d-e)**, the non-linear dimension reduction in SPD-CNN is achieved by alternating the following two steps. Suppose the SPD matrix has been reduced from Sym_N^+ to $Sym_{N_k}^+$ before starting the k^{th} $(k = 1, \dots, K)$ iteration. We first find a bilinear mapping W_k to further reduce the dimensionality of SPD matrix from $N_{k-1} \times N_{k-1}$ to $N_k \times N_k$ by $\mathcal{X}_k = f_b(\mathcal{X}_{k-1}) = W_k \mathcal{X}_{k-1} W_k^T$, where $W_k \in \mathcal{R}^{N_k \times N_{k-1}}$ $(N_k < N_{k-1})$. Similar to the ReLU layer in CNN, the non-linearity is obtained by a hard-thresholding smoothing process in the spectrum domain of the underlying $\mathcal{X}_k$ by $\mathcal{X}_k = f_r(X_k) = U_k max\,(\varepsilon I, \Lambda_k) U_k^T$, where U_k and Λ_k are eigenvectors and the diagonal matrix of corresponding eigenvalues. ε is a pre-defined scalar which controls the regularization of rectifying smaller eigenvalues. At the end of K^{th} iteration, the Log-Euclidean operator [13] is adapted to project $\mathcal{X}_K \in Sym_{N_K}^+$ from the Riemannian manifold of SPD matrix to the d-length vector $v \in \mathcal{R}^d$ by $v = f_g(\mathcal{X}_K) = U_K log(\Lambda_K) U_K^T$, where $log(\Lambda_K)$ is the diagonal matrix of eigenvalue logarithms.

It is clear that the network hyper-parameters Θ of SPD-CNN consists of a set of mapping matrices, i.e., $\Theta = \{W_k | k = 1, \dots, K\}$. Given Θ, we can project the sequence of subject-specific FC matrices $\mathbb{X}_m$ from Sym_N^+ manifold to the stack of vectors $V_m = \left[v_m(t_p)\right]_{p=1}^P$, where each column $v_m(t_p)$ represents the fingerprint of functional connectivity at time t_p for m^{th} subject. Since our goal is to stratify Q cognitive tasks based on V_m for new fMRI scan, we expect the FC fingerprint $v_m(t_p)$ has high similarity to other $v_m(t_{p'})$ $(p' \neq p)$ if t_p and $t_{p'}$ are associated with the same cognitive task, i.e., $y_m(p) = y_m(p')$. Otherwise, their similarity $s_m^{pp'} = s(v_m(t_p), v_m(t_{p'}))$ $(0 \leq s_m^{pp'} \leq 1)$ is required to be as small as possible. In light of this, the loss function ℓ for learning task-specific FC fingerprint is given by:

$$\ell = \sum_{m=1}^{M} \sum_{p,p'=1}^{P} \left(\mathbf{1}_{\{y_m(p) = y_m(p')\}} \left(1 - s_m^{pp'}\right) + \mathbf{1}_{\{y_m(p) \neq y_m(p')\}} \left[s_m^{pp'} - \alpha \right]_+ \right) \quad (1)$$

where the scalar α controls the maximum margin for negative pairs of time points that bear with different functional tasks.

Although we can learn the task-specific FC fingerprints by finding the best network parameter Θ that minimizes the loss function ℓ, a post hoc process (such as clustering) is required to stratify the functional task based on the learned FC fingerprints. In doing so, the gap between feature representation learning and task stratification often yield a sub-optimal result. To solve this issue, we present an integrated solution by concatenating SPD-CNN with a recurrent neural network of mean-shift (MS-RNN), which iteratively groups the learned FC fingerprints V_m into a number of meaningful functional tasks on the vector space $\mathcal{R}^d$.

2.2 Recurrent neural network of mean-shift for functional task stratification

Mean-shift is a non-parametric density estimation technique. The backbone of mean-shift is a set of kernels $h_\delta(v_m(t), v_m(t_p)) = \frac{1}{\sqrt{(2\pi)^d}} e^{-\frac{\delta^2 \cdot \|v_m(t) - v_m(t_p)\|_2^2}{2}}$, which allows

us to delineate the density function of V_m on the vector space $\mathcal{R}^d$ as $\varphi_m(t) = \frac{1}{P}\sum_{p=1}^{P} h_\delta\left(v_m(t), v_m(t_p)\right)$. The kernel width δ is the network parameter that controls the smoothness of the density function $\varphi_m(t)$. Given a set of FC fingerprints V_m of m^{th} subject, the discretized process of mean-shift iteratively repeat the following three steps: **(1)** construct subject-specific kernel matrix $H_m = \psi_h(V_m) = \exp(\delta^2 V_m^T V_m)$; **(2)** calculate the mean-shift $\mathrm{Z}_m = (1-\eta)I + \eta H_m D^{-1}$, where η is the step size and $D = diag(H_m^T \mathbf{1})$ is the diagonal matrix of the row-wise sum of H_m; and **(3)** update V_m by $V_m = \psi_z(V_m) = V_m \mathrm{Z}_m$.

It is clear that the iterative process of mean-shift can be formulated into a recurrent neural network (called MS-RNN in short) Ψ_Δ, where network hyper-parameters include the kernel width $\{\delta_e | e = 1, \ldots, E\}$ in total E iterations. As shown in **Fig. 1(f)**, the distribution of FC fingerprints V_m^E upon the last iteration of mean-shift becomes more and more concentrated at the latent modes than V_m^0 (input to MS-RNN) right after the SPD-CNN. Furthermore, we require the stratification of FC fingerprints to be matched with the functional tasks. Thus, the loss function of our CPD-Net is shown in Eq. (1), where the pair-wise similarity matrix is measured by $s_m^{pp'} = \frac{1}{2}\left(1 + \frac{[v_m(t_p)]^T v_m(t_{p'})}{\|v_m(t_p)\|_2 \|v_m(t_{p'})\|_2}\right)$.

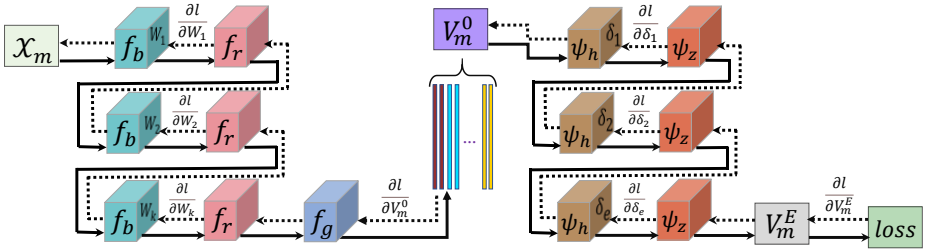

Fig. 2. The feed-forward (solid line) and back-propagation (dashed line) flows in our CPD-Net.

2.3 Back-propagation

Given $\mathbb{X}_m$, the output to our CPD-Net is $V_m^E = \Psi_\Delta(\mathcal{F}_\Theta(\mathbb{X}_m))$. Specifically, the function of SPM-CNN can be formulated as $\mathcal{F} = f_g \circ \underbrace{(f_r \circ f_b) \circ \ldots \circ (f_r \circ f_b)}_{K}$. Likewise, the function of MS-RNN is boiled down to $\Psi = \underbrace{(\psi_z \circ \psi_h) \circ \ldots \circ (\psi_z \circ \psi_h)}_{E}$. Since the loss function (in Eq. 1) eventually examines the mis-stratification based on V_m^E, the back-propagation process starts from the gradient $\frac{\partial l}{\partial V_m^E} = \frac{\partial l}{\partial S}\frac{\partial S}{\partial V_m^E}$, where $\frac{\partial l}{\partial S} = \frac{\partial \ell}{\partial S}\frac{\partial l}{\partial \ell} = (1-2G)\frac{\partial l}{\partial \ell}$ and $\frac{\partial S}{\partial V_m^E} = \frac{\partial S}{\partial V_m^E}\frac{\partial l}{\partial S} = V_m^E \frac{\partial l}{\partial S}$, where G denotes binary indicator matrix, if $y_m(p) = y_m(p')$, $G = 1$, otherwise, $G = 0$. $\frac{\partial l}{\partial \ell} = \frac{1}{P^2}\mathbf{1}_{P\times P}$. Following the gradient chain in [12], it is straightforward to obtain the gradient $\frac{\partial l}{\partial V_m^0}$ at the beginning of MS-

RNN. As shown in **Fig. 2**, the connection between SPD-CNN and MS-RNN is the FC fingerprints V_m^0. Given $\frac{\partial l}{\partial V_m^0}$, we follow the manifold-based operations in [11] to continue the back-propagation in SPM-CNN until we reach $\frac{\partial l}{\partial W_1}$. We use stochastic gradient descent algorithm to optimize network hyperparameters Δ and Θ sequentially.

2.4 Discussion

Due to the subject-to-subject variation of brain structures, it is highly possible that there exist external differences of FC matrices across individuals, which might not be relevant to the state change detection. Therefore, the distribution of FC fingerprints might be distinct from subject to subject on the vector space $\mathcal{R}^d$. However, we would like to argue that our CPD-Net is not sensitive to such inter-subject variations because the role of MS-RNN is to infer the relationship of neighboring time points and then group them into different clusters as separable as possible. In this regard, the location of mode (center of FC fingerprints associated with the same task) in the vector space is not the driving factor of change detection. With that being said, our network is not able to recognize each functional task since we do not enforce inter-subject FC fingerprints of the same functional task bear similar patterns in training our CPD-Net.

3 Experiments

In this section, we evaluated the performance of the proposed CPD-Net for detecting change points on both simulated data and real task-based fMRI data from the HCP (Human Connectome Project). We compare our CPD-Net with two methods, including (1) the spectral clustering method (SC) and (2) the recent clustering method by seeking for density peaks (DP) of the data distribution [14]. In contrast to our method, both counterpart methods first vectorize the functional brain networks and then perform change detection. W use purity score between the ground truth (pre-defined task schedules) and stratified brain states to evaluate the detection accuracy, which has been widely used in the computer vision area for assessing clustering accuracy.

Data description of simulated data. The SimTB toolbox (https://trendscenter.org/software/simtb/) is utilized to generate the simulated fMRI time series with three brain states ($Q = 3$). **Fig. 3** (left) demonstrates three FC matrices at the pre-define cognition stages, where each FC matrix consists of three modules (communities) along the diagonal line (state1 in yellow, state2 in green, state3 in blue). For each possible pair of nodes with the same module, the degree of connectivity is set to one. Otherwise, it is assigned a value of zero concerning cross-module connectivity. Regarding the simulated data, 2000 samples are randomly generated, where each sample opts for two change points ($t_p = 100$ and $t_p = 200$) to separate three states and each state lasts 100 seconds.

Data description on fMRI data from HCP database. We collect in a total of 743 subjects from the HCP database, each with test and retest fMRI scans of the working

memory, which includes 2-back and 0-back task events for body, place, face, and tools, as well as fixation periods. Each task fMRI scan consists of 393 scanning time points and 268 brain regions parcellated by Shen 268 brain region atlas [15]. At the top of **Table 1**, we list the data splitting for training, validation, and testing.

In the following, we first evaluate the contribution of two learning components (SPD-CNN and MS-RNN) in an ablation study in Section 3.1. Then we demonstrate the change detection accuracy on simulated data in Section 3.2, focusing on the influence of sliding window size. In Section 3.3, we specifically evaluate (1) the *accuracy* of change detection, (2) the *replicability* by applying the CPD-Net trained on test data to retest data and vice versa, (3) the *scalability* of change detection by progressively adding attention network (ATN), visual network (VIS), and sensorimotor network (SMN) to the default mode network (DMN) until we use all 268 nodes in the brain network, where the number of nodes in each sub-network is shown in the bottom of **Table. 1**.

Table 1. The description of HCP data in training and testing our CPD-Net.

		training	validation	testing	total
Test		378	47	318	743
Retest		378	47	318	743
Networks	**Total**	DMN	ATN	VIS	SMN
Nodes	**268**	36	22	21	41

3.1 Ablation study

We conduct the ablation study on 743 task-based fMRI data (test and retest data are mixed) by testing all combinations of turning on/off SPD-CNN and MS-RNN. By shutting down SPD-CNN, the input to MS-RNN is the vectorized FC matrices. By shutting down MS-RNN, we use the learned FC fingerprints for clustering. By shutting down both, we simply use the vectorized FC matrix to stratify the time points by data clustering. **Table 2** shows the ablation investigation on the contribution of SPD-CNN and MS-RNN. It is clear that each component plays an important role in change detection, as evidenced by the significant difference after turning off either component.

Table 2. Ablation study of the SPD-CNN and MS-RNN in our CPD-Net. Mean and STD denote the mean and standard deviation of purity for all involved subjects. '×' and '√' denote the absence and presence of the underlying component in the network, respectively.

Case index		1	2	3	4
SPD-CNN		×	×	√	√
MS-RNN		×	√	×	√
Purity	Mean	0.674	0.701	0.729	**0.745**
	STD	0.065	0.041	0.059	**0.040**

3.2 Evaluation of simulated data

We estimate the effect of the window size from 10 to 60 on the performance of FC change detection. At the right panel of **Fig. 3**, we show the detection accuracy (in terms of purity score) results by our CPD-Net (in red), SC (in brown) and DP (in blue), where our CPD-Net outperforms the other two counterpart methods w.r.t. all set window sizes.

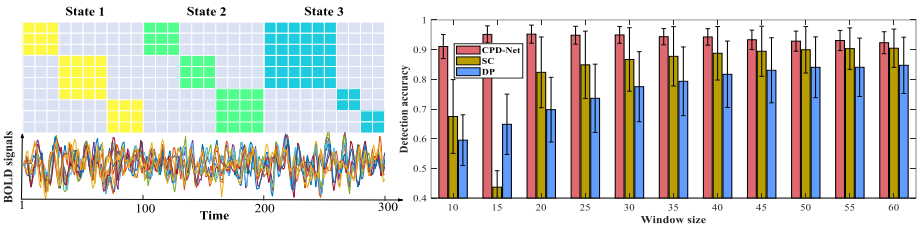

Fig. 3. Left: An example of simulated data with ten brain regions and three brain states. Right: The accuracy of brain state change detection for different window sizes (right).

3.3 Change detection on real task-based fMRI data

Evaluating the accuracy of change detection. In this experiment, we train our CPD-Net for detecting state changes in DMN+ATN network (58 brain regions), where the training and testing data are mixed with test/retest fMRI data. In **Fig. 4(a)**, we show the change detection result of one test data (in the green dash box) and one retest data (in the blue dash box), where the bar plots with different color and height denote the pre-defined time schedule of functional tasks. The automatic detection results by our CPD-Net, SC, and DP are displayed at the bottom of **Fig. 4(a)** with the matched color of ground truth. By examining the temporal alignment between the pre-defined functional tasks and the automatic detection result, our CPD-Net yields more accurate prediction results than the other two methods. In addition, we show the distribution of FC fingerprints on the vector space $\mathcal{R}^d$ (in the sphere) before and after stratification by MS-RNN in **Fig. 4(c)-(d)**, respectively. It is clear that MS-RNN is very effective in grouping the timepoints into isolated modes, which makes change detection much easier.

Next, we evaluate the accuracy of brain state change detection under different window sizes (from 15 to 60). The mean and standard deviation of purity scores are shown in **Fig. 4 (b)** for test and retest data separately since they have different task schedules. Similar to the result of simulated data in **Fig. 3**, our CPD-Net (in red) shows significant improvement ($p < 10^{-4}$) of detection accuracy over SC (in blue) and DP (in brown). Based on this result, we set the sliding window size of 30 in the following experiments.

Evaluating the replicability of change detection. In this experiment, we evaluate the replicability of the brain state change detections between test and retest data where the task schedules are different. Specifically, we examine the test-retest replicability on DMN+ATN networks (58 brain regions). First, we train one CPD-Net using the training

set of the test data only (called CPD-Net-1) and another CPD-Net using the training set of retest data only (called CPD-Net-2), separately (**Table1** shows the specific allocation.). Next, we apply the trained CPD-Net-1 to the testing set of the test data and the testing data of the retest data, where CPD-Net-1 has not seen any instance of retest data in the training stage, and vice versa. We evaluate such test/retest replicability in **Table 3** by showing the change detection accuracy by the scenario of training/testing on the same task schedule versus the scenario of training/testing on different task schedules. By running a two-sample *t*-test between the purity scores of two scenarios, we have not found significant differences by our CPD-Net.

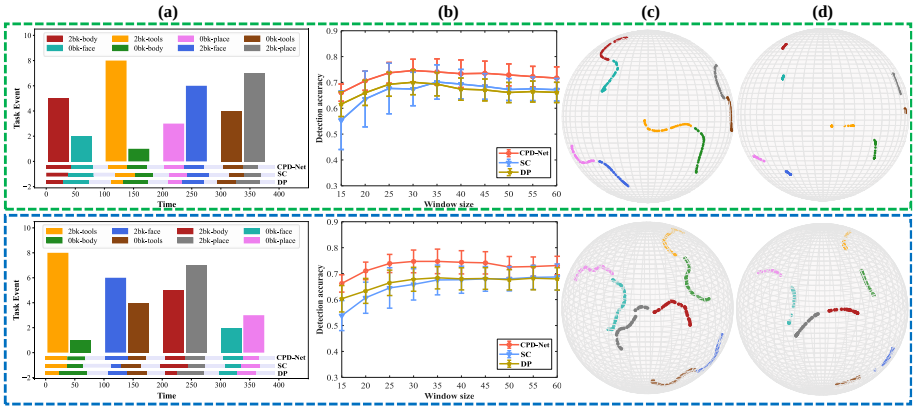

Fig. 4. (a) The typical change detection result by our CPD-Net, SC, and DP methods on test (in green box) and retest data (in blue box). (b) The accuracy of change detection by CPD-Net (in red), SC (in blue), and DP (in brown). (c)-(d) The distribution of FC fingerprints before and after stratification by MS-RNN, where the different colors indicate the different tasks.

Table 3. The detection results for evaluating the replicability of change detection.

		same task schedule vs. different task schedule
CPD-Net 1	Mean	0.7467 vs. 0.7425
	STD	0.0443 vs. 0.0402
	p-value	0.7459
CPD-Net 2	Mean	0.7471 vs. 0.7440
	STD	0.0438 vs. 0.0457
	p-value	0.8249

Evaluating the scalability of change detection. We evaluate the detection accuracy of change detection methods regarding different network sizes. To this end, we increase the number of network dimensions by successively adding nodes from sub-networks like default mode network (DMN), attention network (ATN), visual network (VIS) and sensorimotor network (SMN) until involving the whole brain regions. The involved nodes at different network dimensions are illustrated in the top of **Fig. 5**, and the corresponding detection results conducted on test and retest data are shown in **Fig. 5** (middle and bottom). Our CPD-Net consistently outperforms all the comparison

methods on different network dimensions, where the red '*' denotes the significant improvement ($p < 10^{-4}$) over the other two methods. Our CPD-Net is more scalable to be expanded to large-scale brain networks than all comparison methods.

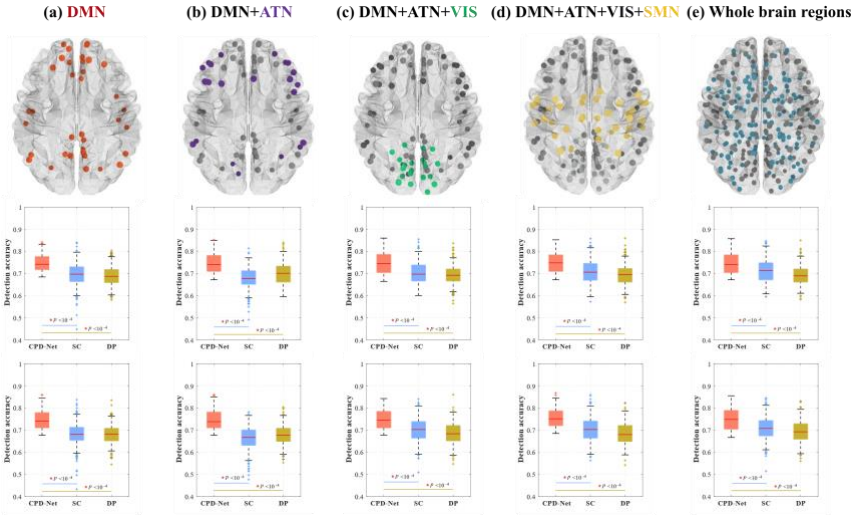

Fig. 5. The detection accuracy for different network dimensions. (a) – (e) progressively include DMN, ATN, VIS, SMN and the whole brain.

4 Conclusion

In this study, we devised a novel deep change point detection network (CPD-Net) by learning task-specific functional connectivity fingerprints for functional brain network analysis. The functional connectivity matrices of our model are constructed by covariance matrices derived from the BOLD signals, thus the input of our CPD-Net is a series of SPD matrices. Our CPD-Net not only can preserve the preferable intrinsic geometric properties of functional connectivity matrices by the SPD-CNN module, but also refine the modes of the learned FC fingerprints by MS-RNN module to distinguish the different brain states. Different from most of the existing methods, our CPD-Net can learn more discriminating information that can represent the relationship of neighboring time points, instead of optimizing parameters for each new subject. Extensive experiments demonstrate that our CPD-Net can be effectively detecting the change of functional brain states with preferable change detection accuracy.

5 References

1. Buckner, R.L., Krienen, F.M., Yeo, B.T.T.: Opportunities and limitations of intrinsic functional connectivity MRI. Nature Neuroscience 16, 832-837 (2013)

2. Filippi, M., Spinelli, E.G., Cividini, C., Agosta, F.: Resting State Dynamic Functional Connectivity in Neurodegenerative Conditions: A Review of Magnetic Resonance Imaging Findings. Frontiers in neuroscience 13, 657-657 (2019)
3. Xu, Y., Lindquist, M.: Dynamic Connectivity Detection: an algorithm for determining functional connectivity change points in fMRI data. Frontiers in Neuroscience 9, (2015)
4. Cribben, I., Haraldsdottir, R., Atlas, L.Y., Wager, T.D., Lindquist, M.A.: Dynamic connectivity regression: determining state-related changes in brain connectivity. Neuroimage 61, 907-920 (2012)
5. Li, H., Fan, Y.: Identification of Temporal Transition of Functional States Using Recurrent Neural Networks from Functional MRI. Med Image Comput Comput Assist Interv 11072, 232-239 (2018)
6. Li, H., Satterthwaite, T.D., Fan, Y.: Large-scale sparse functional networks from resting state fMRI. Neuroimage 156, 1-13 (2017)
7. Feldt, S., Waddell, J., Hetrick, V.L., Berke, J.D., Zochowski, M.: Functional clustering algorithm for the analysis of dynamic network data. Physical review. E, Statistical, nonlinear, and soft matter physics 79, 056104 (2009)
8. Lin, Y., Laurienti, P., Wu, G.: Detecting Changes of Functional Connectivity by Dynamic Graph Embedding Learning. 23rd Internatinal Conference on Medical Image Computing and Computer Assisted Intervention (MICCAI 2020), Lima, Peru (2020)
9. Biswal, B., Yetkin, F.Z., Haughton, V.M., Hyde, J.S.: Functional connectivity in the motor cortex of resting human brain using echo-planar MRI. Magnetic resonance in medicine 34, 537-541 (1995)
10. Dai, M., Zhang, Z., Srivastava, A.: Analyzing Dynamical Brain Functional Connectivity as Trajectories on Space of Covariance Matrices. IEEE Transactions on Medical Imaging 39, 611-620 (2020)
11. Huang, Z., Gool, L.V.: A riemannian network for SPD matrix learning. Proceedings of the Thirty-First AAAI Conference on Artificial Intelligence, pp. 2036–2042. AAAI Press, San Francisco, California, USA (2017)
12. Kong, S., Fowlkes, C.: Recurrent Pixel Embedding for Instance Grouping. In: 2018 IEEE/CVF Conference on Computer Vision and Pattern Recognition, pp. 9018-9028. (Year)
13. Arsigny, V., Fillard, P., Pennec, X., Ayache, N.: Geometric Means in a Novel Vector Space Structure on Symmetric Positive-Definite Matrices. SIAM Journal on Matrix Analysis and Applications 29, 328-347 (2007)
14. Rodriguez, A., Laio, A.: Clustering by fast search and find of density peaks. Science 344(6191), 1492-1496 (2014)
15. Shen, X., Tokoglu, F., Papademetris, X., Constable, R.T.: Groupwise whole-brain parcellation from resting-state fMRI data for network node identification. NeuroImage 82, 403-415 (2013)